JOURNAL OF VIROLOGY, Oct. 2010, p. 10653–10660 Vol. 84, No. 20
0022-538X/10/$12.00 doi:10.1128/JVI.00848-10

The Viral Latency-Associated Nuclear Antigen Augments the B-Cell Response to Antigen *In Vivo*▽

Sang-Hoon Sin, Farnaz D. Fakhari, and Dirk P. Dittmer*

Department of Microbiology and Immunology, Lineberger Comprehensive Cancer Center, Center for AIDS Research, University of North Carolina at Chapel Hill, Chapel Hill, North Carolina 27599-7290

Received 21 April 2010/Accepted 28 July 2010

Gammaherpesviruses, including Kaposi sarcoma-associated herpesvirus (KSHV), establish latency in B cells. We hypothesized that the KSHV latency-associated nuclear antigen (LANA/orf73) provides a selective advantage to infected B cells by driving proliferation in response to antigen. To test this, we used LANA B-cell transgenic mice. Eight days after immunization with antigen without adjuvant, LANA mice had significantly more activated germinal center (GC) B cells ($CD19^+$ PNA^+ $CD71^+$) than controls. This was dependent upon B-cell receptor since LANA did not restore the GC defect of CD19 knockout mice. However, LANA was able to restore the marginal zone defect in CD19 knockout mice.

B-cell receptor (BCR) signaling is modulated at multiple levels. CD19 impinges on antigen-dependent B-cell survival, proliferation, and differentiation through direct interaction with the BCR molecule (24, 51). Phosphatase and tensin homolog deleted on chromosome 10 (PTEN) and Burton's tyrosine kinase (BTK), as well as others, modulate cytoplasmic second messenger and subsequent adaptor-dependent BCR signaling steps (34). In fact, loss of PTEN can compensate for the loss of CD19 function (6). We find that a viral protein of a B-cell tropic human herpesvirus similarly modulates BCR signaling *in vivo*, resulting in hyperactive naive B cells. This viral protein is nuclear localized, and thus far most of its functionality has been attributed to transcriptional regulation and sequence-specific DNA binding. This protein is not an oncogene as defined by the classic, cell autonomous transformation assay. Our *in vivo* data show that it is a subtler regulator of B-cell differentiation and suggest a novel mechanism as to how immunotropic viruses modulate BCR signaling to further the preferential survival and expansion of virally infected host cells *in vivo*.

Kaposi sarcoma-associated herpesvirus (KSHV) is a B-cell tropic human tumor virus. In addition to causing Kaposi sarcoma, it is also the causative agent of a type of post-germinal center (GC) diffuse large B-cell lymphoma (DLBCL), and primary effusion lymphoma (PEL), as well as the plasmablastic variant of multicentric Castleman's disease (MCD) (9, 10). KSHV can be found in peripheral blood, mature, $CD19^+$ B cells (15, 37). During asymptomatic, latent persistence in $CD19^+$ B cells, as well as in 99% of PEL cells in culture, only the latency-associated nuclear antigen (LANA) and a few other viral latent genes in the LANA latency locus are expressed (18, 20, 27, 45).

We previously generated transgenic mice, which express LANA in $CD19^+$ mature B cells (21). In these mice LANA is under the control of its own viral promoter, which is B cell specific (28). LANA transgenic mice exhibit an activated mature B-cell phenotype, as evidenced by the expansion of $CD19^+$ IgM^+ IgD^+ FSC^{hi} splenic B cells.

Functionally, B cells can be divided into follicular B cells (FL cells), which respond to T-cell-dependent antigens, and marginal zone B cells (MZ cells), which respond to multivalent, so-called T-cell-independent antigens. MZ cells also drive the primary (days 2 to 4) low-affinity B-cell response to antigen (reviewed in reference 26). Both populations require BCR engagement and CD19 for proliferation and differentiation.

FL cells require T-cell help in their response to monovalent antigens, e.g., the hapten 4-hydroxy-3-nitrophenylacetyl (NP). The B-cell–T-cell interaction takes place in the germinal centers (GC). Note that there are three steps in follicular B-cell activation: (i) antigen binding and transformation to activated B-cell blasts, which are FSC^{hi} and express the CD71 and CD68 activation markers (31); (ii) T-cell-dependent activation and migration into the GC; and (iii) T-cell-dependent class switching, GC exit, and differentiation (reviewed in reference 1).

MZ B cells do not necessarily require T-cell help, although they do respond to T-cell-dependent antigens and are responsible for the primary IgM response (54). In addition, strong, multivalent antigens are thought to multimerize BCR molecules to such an extent that MZ cell activation is induced independently of direct T-cell contact (16, 35).

To test whether the LANA-induced hyperplasia is dependent on BCR-transmitted activation signals, we crossed LANA transgenic mice to isogenic $CD19^{-/-}$ mice (19, 24, 51). We found that the LANA transgene could not rescue the GC B-cell deficiency of $CD19^{-/-}$ mice. However, LANA was able to rescue the MZ defect in $CD19^{-/-}$ mice. We further found that LANA augmented the primary B-cell response to acute antigen, a finding consistent with a model in which LANA lowers the threshold for BCR-dependent B-cell activation, proliferation, and survival.

In the widest sense, these *in vivo* observations suggest that antigen exposure fosters latent persistence of B-cell-tropic her-

* Corresponding author. Mailing address: Department of Microbiology and Immunology, Lineberger Comprehensive Cancer Center, Center for AIDS Research, University of North Carolina at Chapel Hill, CB#7290, 715 Mary Ellen Jones Bldg, Chapel Hill, NC 27599-7290. Phone: (919) 966-7960. Fax: (919) 962-8103. E-mail: ddittmer@med.unc.edu.

▽ Published ahead of print on 4 August 2010.

pesviruses, analogous to the way in which microbial translocations foster T-cell activation and HIV replication (8). Previously, it was reported that transgenic expression of the Epstein-Barr virus (EBV) LMP1 protein accelerated extrafollicular B-cell differentiation *in vivo* mimicking CD40 signaling (60), that EBV LMP2A enhances B-cell responses (4, 56), and that murine herpesvirus 68 (MHV68) coinfection fosters macrophage responses to bacterial antigens (7). The present study is the first demonstration that B cells expressing a KSHV viral protein displayed enhanced response to a T-dependent antigen.

MATERIALS AND METHODS

Mice. Transgenic mice expressing KSHV LANA were previously described (21). CD19 knockout mice [C.129P2-*Cd19*$^{tm1(cre)Cgn}$/J] were purchased from the Jackson Laboratory (Bar Harbor, ME). LANA$^{+/-}$ CD19 knockout mice were obtained by breeding LANA transgenic mice with CD19 knockout mice. Mice were maintained under pathogen-free conditions using ventilated cages. Animals were injected intraperitoneally with 100 μg of 4-hydroxy-3-nitrophenylacetyl–keyhole limpet hemocyanin (NP-KLH; Biosearch Technologies, Inc., Novato, CA) in 200 μl of phosphate-buffered saline (PBS). All experiments were approved by the Institutional Animal Care and Use Committee (IACUC) at the University of North Carolina at Chapel Hill.

Genotyping. Tail DNA was isolated by using a Wizard SV genomic DNA kit (Promega). A PCR was set up in a volume of 20 μl with 2× SYBR PCR mix (Applied Biosystems, Foster City, CA), 1.7 ng of genomic DNA, and 125 nmol of primers. PCR was performed according to the following protocol: 5 min at 94°C, followed by 40 cycles of 15 s at 94°C, 30 s at 55°C, and 1 min at 72°C for CD19 primers (5′-CCTCTCCCTGTCTCCTTCCT-3′ and 5′-TGGTCTGAGAC ATTGACAATCA-3′) and Cre primers (5′-GCGGTCTGGCAGTAAAAACTA TC-3′ and 5′-GTGAAACAGCATTGCTGTCACTT-3′). PCRs were preheated for 5 min at 94°C, followed by 40 cycles of 10 s at 94°C and 30 s at 62°C for LANA primers (2454F [TGGCCCATCTCGCGAATA] and 2581R [GGACCGGTGG TTGTTGGTAT]). The PCR products for CD19 and Cre were mixed together and run on one lane on a 3% agarose gel for each mouse. A 100-bp molecular weight marker (New England Biolabs, Ipswich, MA) was loaded on a separate lane on each gel. PCR amplification for KSHV LANA and murine apoB was conducted as described previously (21).

B-cell isolation and proliferation assay. B cells were purified from a mouse spleen immunized with NP-KLH via elimination of non-B cells using an EasySep mouse B-cell enrichment kit (Stemcell, Vancouver, Canada). The percentage of CD19$^+$ enriched B cells was 96 to 97%, when assessed by fluorescence-activated cell sorting. Purified B cells were cultured in RPMI 1640 medium supplemented with 20% fetal bovine serum, 2 mM L-glutamine, penicillin (0.05 μg/ml), and streptomycin (5 U/ml) (Invitrogen, Inc., Carlsbad, CA) at 37°C under 5% CO_2. Purified B cells were stimulated with 50 μg of lipopolysaccharide (LPS)/ml (from *Escherichia coli* O111:B4; Invivogen) or left unstimulated in the aforementioned culture medium containing interleukin-4 (IL-4; 10 U/ml; Peprotech, Rocky Hill, NJ) and IL-5 (1 ng/ml; Peprotech). Proliferation of the B cells was measured with CFSE (carboxyfluorescein diacetate succinimidyl ester; Invitrogen) labeling. Briefly, B cells were labeled with 1 μM CFSE, cultured for 4 days, and analyzed by flow cytometry. Live cells were gated by using a Live/Dead fixable dead cell stain kit (Invitrogen).

Flow cytometry. Single-cell suspensions of mouse spleen were isolated as described previously (21). Flow cytometry analysis was performed by using CyAn (Beckman-Coulter, Fullerton, CA). Further analysis was conducted with FlowJo (version 7.2.5; Tree Star, Inc., Ashland, OR) and R version 2.8.0 (2008-10-20).

Antibodies. Alexa Fluor 488-conjugated anti-B220 (clone RA3-6B2), fluorescein isothiocyanate (FITC)-conjugated anti-mouse activation antigen GL7 (clone GL7, Ly77), anti-mouse IgD (clone 11-26c.2a), phycoerythrin (PE)-conjugated anti-mouse CD21/CD35 (clone 7G6), anti-mouse IgM (clone R6-60.2), and PE/Cy5.5-conjugated anti-mouse CD45R (clone RA3-6B2) monoclonal antibodies were purchased from BD Biosciences (Franklin Lakes, NJ). Alexa Fluor 555-conjugated streptavidin, allophycocyanin (APC)-conjugated anti-mouse CD19 (clone 6D5), anti-mouse CD23 (clone B3B4), streptavidin, FITC-conjugated anti-mouse CD24 (clone CT-HAS), anti-mouse CD69 (clone H1.2F3), and PE-conjugated anti-mouse CD86 (clone RMMP-2) were obtained from Invitrogen (Camarillo, CA). Biotinylated metallophilic macrophages antibody (MOMA1) was obtained from Abcam (Cambridge, MA). Biotinylated peanut agglutinin (PNA) was purchased from Vector Laboratories (Burlingame, CA). Anti-GL7 antibody was purchased from eBioscience (San Diego, CA).

Immunohistochemistry. Spleens were removed, fixed in 10% neutral buffered formalin, embedded in paraffin, and processed by routine methods to obtain 5-μm sections. Dewaxed sections were microwaved in 1 mM EDTA (pH 8.0) for PNA staining for 15 min, cooled, treated with 3% H_2O_2, blocked with blocking solution (10% horse serum, 5% bovine serum albumin, and 0.3% Triton X-100 in PBS), and incubated overnight with the appropriate primary antibody. Detection was performed with a VectaStain ABC kit, a Vector DAB peroxidase substrate kit for PNA, and a Vector *Nova*RED peroxidase substrate kit for GL7 (Vector Laboratories, Inc.).

For MOMA1 detection, spleens were removed and mounted with tissue freezing medium. Cryosections (6 μm) were cut with a cryotome (Leica CM1850 UV), air dried, fixed in cold acetone for 10 min, washed with PBS, dried, and stored in an airtight box at −80°C. The slides were dried in air before use. Immunohistochemical assays were done as described previously (21) with modifications. Briefly, cryosections were fixed in cold acetone for 10 min at 4°C, air dried, and rehydrated in PBS. Slides were incubated for 15 min with a blocking solution consisting of 10% (vol/vol) fetal bovine serum in PBS. Sections were washed three times in a washing buffer (PBS containing 0.05% Triton X-100) and stained for 18 h at 4°C with the appropriate primary antibodies. Sections were washed again and incubated for 2 h with secondary antibody. Finally, slides were washed with a washing buffer three times and mounted in VectaShield mounting medium (Vector Laboratories, Inc.).

Statistical analysis. We used the R statistical package (version 2.10.1) for all of our calculations. We used a *t* test or nonparametric Wilcoxon signed rank test for comparisons between two groups. Both yielded consistent results. We used $n \geq 5$ animals per group. For experiments involving two factors (transgene and treatment), we used analysis of variance (ANOVA) to establish overall and individual factor significance levels. This was possible since our experimental design was balanced with regard to its statistical properties.

RESULTS

LANA augments the acute B-cell response to antigen. We previously observed mature (CD19$^+$ IgD$^+$ IgM$^+$) B-cell hyperactivation and hyperplasia in our B-cell-specific KSHV LANA transgenic mice. We hypothesized that LANA lowers the threshold of mature B cells to respond to antigens. To test this hypothesis, we injected mice once with the NP-KLH model antigen or saline (36, 51). Eight days later, which is before the onset of affinity maturation (reviewed in reference 1), we investigated the primary B-cell response in the spleen. Importantly, this experiment did not use any adjuvant and thus mimicked natural, weak antigen exposure.

Activated B cells were defined as CD19$^+$ PNA$^+$ CD71^{hi} and quantified by flow cytometry (Fig. 1A). PNA is a well-established marker for activated B cells (51), and CD71 (transferrin receptor) is an early lymphocyte activation marker (31). CD71 is also expressed on PEL cells (5). Mock-treated C57BL/6 mice ($n = 10$) had background levels of activated B cells (mean = 24.48%). NP-KLH immunized C57BL/6 mice ($n = 5$) showed the expected increase in activated B cells (mean = 40.98%). LANA transgenic mice in the absence of specific immunization presented with the same frequency of activated B cells as purposely immunized nontransgenic mice ($n = 10$, mean = 41.19%). LANA transgenic mice also upregulated the CD68 activation marker on CD19 B cells in the absence of specific immunization (data not shown). Upon immunization with NP-KLH the number of activated GC B cells increased further in the LANA transgenic mice ($n = 6$, mean = 46.40%). It increased above the background frequency in LANA transgenic mock-treated mice and above the frequency of nontransgenic, immunized mice. Some of the NP-KLH immunized LANA transgenic mice had the highest number of activated GC B

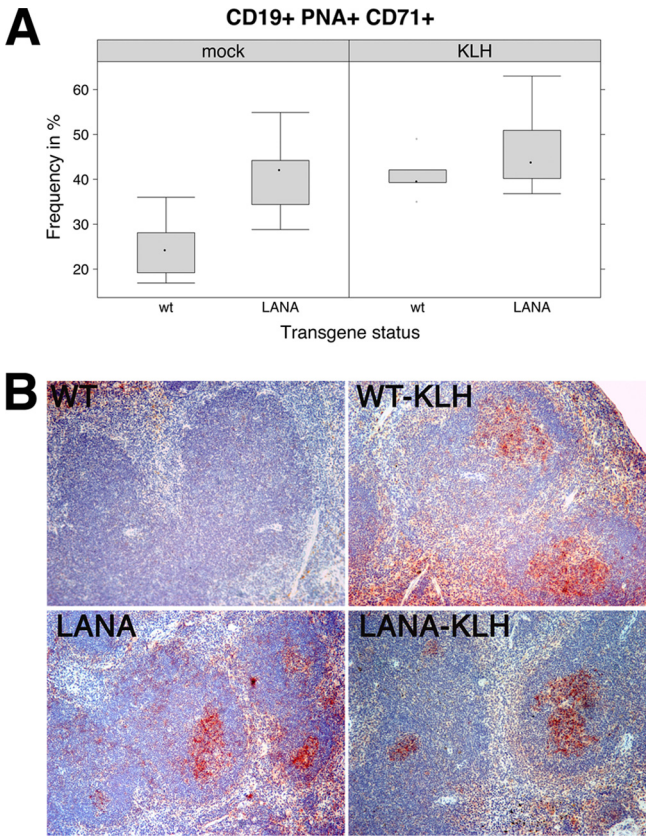

FIG. 1. LANA augments the B-cell response to immunization. (A) Box plot of flow cytometry results. The frequency of triple-positive ($CD19^+$ PNA^+ $CD71^+$) among $CD19^+$ was determined and plotted. The transgene status is shown on the bottom, and the treatment is shown at the top of the graph. A dot indicates the median, the box indicates the interquartile range (IQR), bars denote the range, and open dots denote outliers ($>1.5 \times$ IQR). NP-KLH, 4-hydroxy-3-nitrophenylacetyl–keyhole limpet hemocyanin; LANA, LANA transgenic; WT, wild type. (B) Immunohistochemistry against GL7 antigen (brown) and hematoxylin (blue). Shown are representative images of spleen (magnification, ×40) for wild-type (WT), LANA transgenic (LANA), wild-type NP-KLH-immunized (WT-KLH), and LANA NP-KLH-immunized (LANA-KLH) animals.

cells of all animals in this experiment (maximum of 63%). ANOVA showed a significant difference between all groups. Based on multivariate analysis, both the LANA transgene ($P \leq 0.00001$) and NP-KLH immunization ($P \leq 0.002$) contributed independently and additively to the observed phenotypes. This demonstrates that LANA augments the primary B-cell response to background and experimental antigens.

We verified this result by using immunohistochemistry for the late GC marker GL7 (Fig. 1B). GL7 is expressed in centrocytes (23). It is a more stringent marker than PNA or CD71 since it identifies cells that completed the GC reaction. We did not observe any $GL7^+$ foci in mock-treated C57BL/6 mice. $GL7^+$ foci, i.e., GC, were induced by NP-KLH in C57BL/6 mice. LANA transgenic mice exhibited $GL7^+$ foci in the absence of specific antigen stimulation, a finding consistent with a lower activation threshold to environmental antigen exposure in LANA transgenic compared to wild-type mice. NP-KLH-immunized LANA transgenic mice exhibited $GL7^+$ GC, which is consistent with acute antigen exposure, although this analysis did not detect a difference in the size or frequency of GC in KLH-immunized compared to nonimmunized LANA transgenic mice.

We interpret these data to mean that LANA lowers the threshold of B-cell activation. In the absence of specific immunization, any mature B-cell with a BCR of any affinity to any environmental or chance antigen can become activated. In the absence of LANA this signal is short-lived or never reaches the threshold to induce a proliferative phenotype or GC reaction. In the presence of LANA this threshold is lowered.

If LANA lowers the activation threshold of naive B cells, leading to continual activation, then this may lead to B-cell exhaustion. We therefore investigated the proliferative response of purified CD19 positive B cells in culture (Fig. 2). Since NP-KLH is a T-dependent antigen, we could not use NP to stimulate purified B cells. Instead, we tested the hypothesis that purified B cells from LANA or wild-type mice respond equally well to the standard polyclonal stimulus LPS. LPS is used as positive control in many B-cell proliferation studies. We purified B cells by negative selection to avoid inadvertently activating them. Purified B cells were stimulated with 50 μg of LPS (from *Escherichia coli* O111:B4)/ml as published elsewhere (40), and proliferation was determined by CFSE assay over 4 days.

B cells from LANA transgenic mice proliferated more in response to LPS than B cells from nontransgenic littermates (Fig. 2A and C). The difference was statistically significant to $P \leq 0.005$ using the Wilcoxon rank sum test (Fig. 2E). This result corroborated our *in vivo* data that LANA augmented the B-cell response. B cells from NP-KLH-immunized mice responded equally well to LPS in culture, whether derived from LANA transgenic or wild-type mice (Fig. 2B and D). There was no statistically significant difference in their responses. We interpret these data to mean that even though LANA induces hyper-responsiveness in B cells *in vivo*, this does not lead to exhaustion.

LANA does not restore the B-cell defect in CD19 knockout mice. A key proposition of our threshold modulation model is that LANA-associated B-cell hyperactivation is a BCR-dependent rather than a cell-autonomous phenotype. We therefore sought to determine whether LANA could complement an absolute defect in BCR signaling as seen in CD19-deficient mice. CD19 is part of the BCR signaling complex (51). CD19 is not required for B cells to mature into IgM^+ IgD^+ cells, but the lack of CD19 manifests itself by the absence of GC (19, 61). $CD19^{-/-}$ mice also lack MZ cells. $CD19^{-/-}$ mice in the C57BL/6 background were obtained from Jackson Labs (Fig. 3A).

The double heterozygous F_1 mice ($LANA^{+/-}$ $CD19^{+/-}$) exhibited the LANA-associated B-cell hyperplasia phenotype similarly to $LANA^{+/-}$ $CD19^{+/+}$ homozygous animals, as determined by the frequency of $B220^+$ IgD^+ PNA^+ cells (Fig. 3B, right side). We used B220 as a B-cell marker here to capture any and all B cells in the $CD19^{-/-}$ mice. The $CD19^{-/-}$ $LANA^{+/-}$ transgenic animals seemed to have slightly higher numbers of activated IgD^+ cells (Fig. 3B, left side). However, within the group of $CD19^{-/-}$ animals this difference was not statistically significant. ANOVA incorporating all animals ($n = 30$) established that LANA conferred a proliferative pheno-

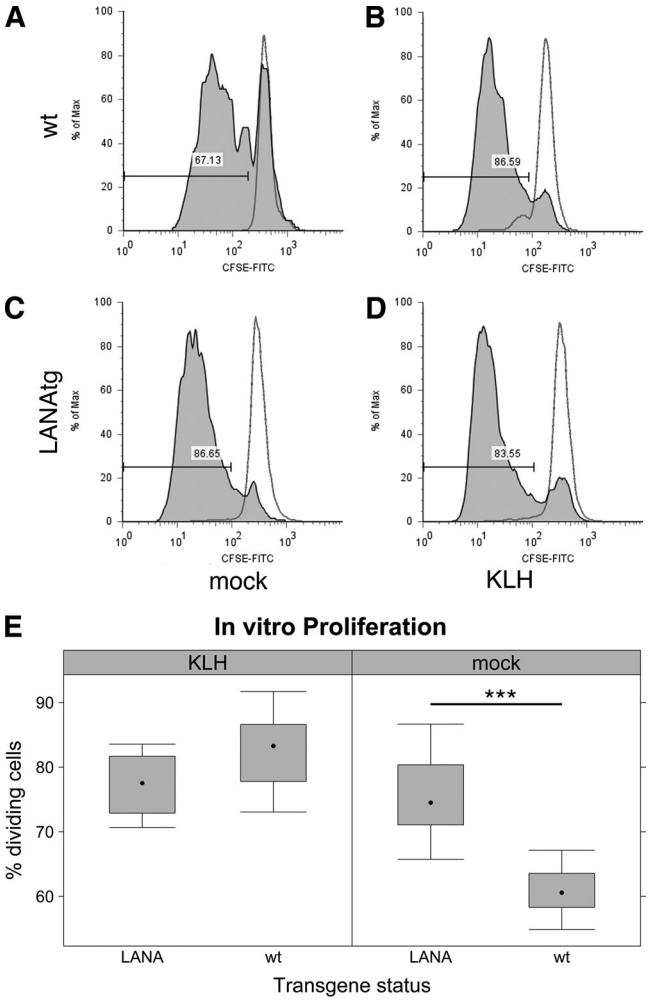

FIG. 2. LANA augments the proliferative capacity of B cells in culture. (A to D) Examples of flow cytometric analysis of purified cultured B cells labeled with CFSE after 4-day stimulation with LPS (gray density) or nonstimulation control (open diagram). Stimulation is measured by the fraction of cells that lose fluorescent intensity. The horizontal line (and number) indicates the gate that was used for quantification. The CFSE fluorescence intensity is shown on the horizontal axis, and the number of cells as a percentage of the maximum is shown on the vertical axis. Results with B cells from LANA transgenic mice are shown in panels C and D, and results from wild-type littermate control animals are shown in panels A and B. Animals in panels B and D were *in vivo* stimulated by NP-KLH immunization prior to harvest. (E) Box-and-whisker plot of the results from multiple animals. A dot indicates the median, a box indicates the interquartile range (IQR), bars indicate the range, and open dots denote outliers (>1.5 × IQR). The three asterisks indicate a significant difference between groups of six LANA and six wild-type mice at $P \leq 0.005$ as determined by using the Wilcoxon rank sum test.

type ($P \leq 10^{-6}$), even in CD19$^{+/-}$ hypomorphic animals, and that the lack of CD19 conferred the expected loss of IgD^{+} PNA^{+} cells ($P \leq 5 \times 10^{-15}$). LANA, however, was not able to overcome this, the predominant phenotype.

As determined by hematoxylin and eosin (H&E) staining of spleen sections, the LANA$^{+/-}$ CD19$^{-/-}$ animals shared the phenotype of the CD19$^{-/-}$ parent. Figure 3C and D show spleen sections of a C57BL/6 (LANA$^{-/-}$ CD19$^{+/+}$) mouse with clearly demarcated, isolated GC and MZ regions between the red and white pulp. Figure 3E and F show spleen sections of a LANA transgenic mouse ((LANA$^{+/-}$ CD19$^{+/+}$). As we previously observed in 100% of LANA transgenic mice, the spleen is disorganized, with enlarged, irregular GC and expanded MZ. Often, the GC run into each other, and the red pulp zone is diminished. Figure 3G and H show spleen sections of a LANA$^{+/-}$ CD19$^{-/-}$, which are indistinguishable from transgene-negative CD19$^{-/-}$ mice (19; data not shown). Note the absence of GC (light zone), a sharply shrunk MZ around them, but the presence of clearly demarcated, isolated foci, unlike the hyperplasia seen in the presence of CD19. We conclude that LANA was not able to compensate for the lack of CD19 in GC development and that LANA-induced B-cell hyperactivation requires BCR signaling.

To visualize the GC, we used PNA as a marker (Fig. 3I to K). Wild-type mice show a few, very small PNA-positive staining foci. LANA transgenic mice show many, extended, irregular PNA-positive staining foci, as well as individual PNA-positive cells outside of organized follicles. The LANA$^{+/-}$ CD19$^{-/-}$ exhibited no PNA positivity, either as foci or as individual cells. This represents the CD19$^{-/-}$ phenotype. The presence of the LANA transgene did not rescue the GC defect in CD19$^{-/-}$ mouse.

To independently verify these results, we analyzed a second cohort of age-matched 15- to 21-week-old LANA$^{+/-}$ CD19$^{-/-}$ mice ($n = 9$) with LANA$^{-/-}$ CD19$^{-/-}$ ($n = 6$) mice by using multicolor flow cytometry analysis (Table 1). CD19$^{-/-}$ mice develop normal follicular B-cell (B220^{+} CD21^{+} CD23^{+} CD24^{lo}) compartment (41), and LANA$^{+/-}$/CD19$^{-/-}$ mice at 15 to 21 weeks old showed a similar percentage of follicular B cells as LANA$^{-/-}$/CD19$^{-/-}$ mice (Table 1). Comparing LANA$^{+/-}$/CD19$^{-/-}$ mice with LANA$^{-/-}$/CD19$^{-/-}$ (F_2) revealed no GC formation associated with LANA expression in the absence of CD19 signaling (Table 1).

LANA restores the MZ defect in CD19 knockout mice partially. CD19$^{-/-}$ mice show severe reduction in MZ B cells (B220^{+} CD21^{hi} CD23^{-} CD24^{+}) (19, 35, 42, 51). We found increased MZ cells in LANA$^{+/-}$/CD19$^{-/-}$ mice (3.46% ± 1.08, $n = 9$) compared to LANA$^{-/-}$/CD19$^{-/-}$ mice (2.05% ± 0.45, $n = 6$). Representative results are shown in Fig. 4A and B. The percentage of MZ B cells in the age-matched LANA$^{-/-}$/CD19$^{+/-}$ littermates controls was 8.71% ± 2.16. Although MZ comprise only a minor fraction of B cells in normal mice, we were able to detect a statistically significant difference ($P \leq 0.003$ using ANOVA) using sets of three-color (B220^{+} CD21^{hi} CD23^{-}, Fig. 4C) and four-color flow cytometry markers (B220^{+} CD21^{hi} CD23^{-} CD24^{+}; data not shown). This demonstrates that LANA can rescue the CD19 deficiency-associated defect in the MZ B-cell development partially.

We confirmed this result by using immune fluorescence microscopy assay (IFA). Spleens from age-matched mice were stained using MOMA-1, a marker for marginal zone macrophages, and B220, a pan-B-cell marker. We did not use CD19 as a B-cell marker, since of course CD19 would be absent in the CD19$^{-/-}$ background. In wild-type mice, MOMA-1 marks the middle of the marginal zone (Fig. 4D, wt). B cells are present in between MOMA-1-positive macrophages, within the MOMA-1 ring demarking the GC center and, importantly,

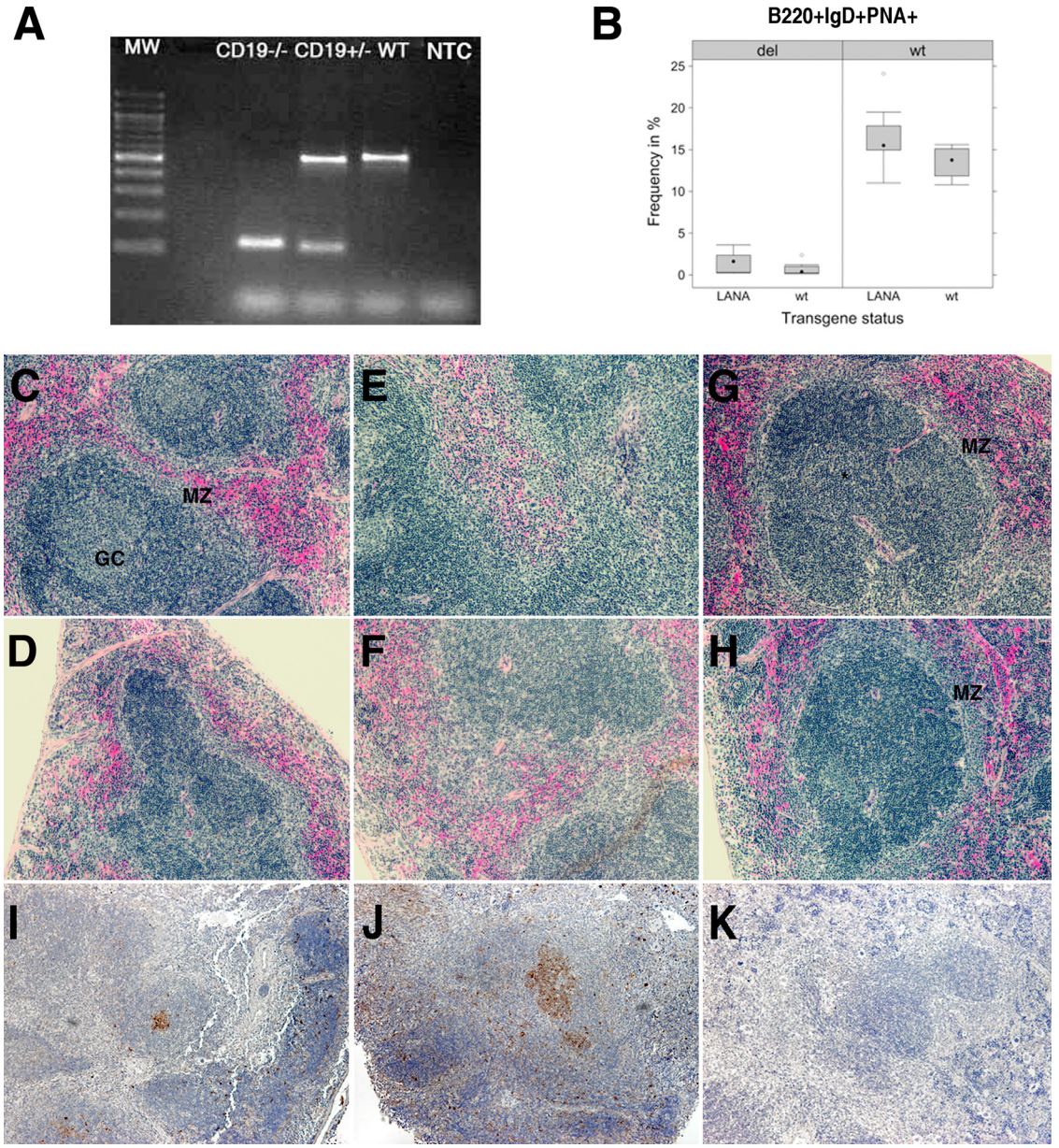

FIG. 3. LANA does not complement the B-cell deficiency in CD19 knockout mice. (A) Shown is a representative picture of an ethidium bromide-stained 1% agarose–TAE gel of PCR products using mouse tail DNA. One hundred-base-pair molecular weight markers are shown on the left (MW); inferred genotypes are shown at the top. WT, wild type; NTC, nontemplate control. (B) Box plot of flow cytometry results (n = 30, animals are not incorporated in Table 1). The frequency of triple-positive ($B220^+$ IgD^+ PNA^+) was determined and plotted. The LANA transgene status is shown at the bottom, and the CD19 status is shown at the top of the graph. Dot indicates the median, a box indicates the interquartile range (IQR), bars indicate the range, and open dots denote outliers (>1.5 × IQR). del, deletion for CD19 ($CD19^{-/-}$); wt (top), $CD19^{+/+}$; LANA, LANA transgenic; wt, wild-type ($LANA^{-/-}$). The morphology of the spleen in wild-type (C and D), LANA transgenic (E and F), and $CD19^{-/-}/LANA^{+/-}$ (G and H) mice is shown. Representative H&E-stained images are presented. The upper row is at ×100 magnification, the lower row is at ×40 magnification. MZ, marginal zone, GC, germinal center. The asterisk in panel G denotes the absence of GC in $CD19^{-/-}/LANA^{+/-}$ mice. Immunohistochemistry for PNA (brown) counterstained with hematoxylin (blue) was performed. Representative sections for wild-type (I), LANA transgenic (J), and $CD19^{-/-}/LANA^{+/-}$ (K) mice are presented.

also outside the MOMA-1 ring. In $CD19^{-/-}$ mice, MOMA-1 staining was reduced and no B220-positive cells were noticeable adjacent to the MOMA-1-positive cells (Fig. 4D, $CD19^{-/-}$). Furthermore, the B220-positive clusters were fewer and smaller compared to wild-type mice. This represents the typical phenotype of $CD19^{-/-}$ mice (19, 48, 51). The presence of the LANA transgene rescued the marginal zone B-cell deficiency of the $CD19^{-/-}$. Corroborating our quantitative, multiparameter flow cytometric analysis, the immune fluorescence image now revealed many more MOMA-1-positive cells in typical MZ morphology (Fig. 4D, $CD19^{-/-}$ × LANA). Also, $B220^+$ B cells (green) can now be observed adjacent to MOMA-1 MZ

TABLE 1. Summary of cell surface marker analysis of wild-type, CD19-deficient, and LANA-transgenic, CD19-deficient mice

Class	Marker	B-cell subpopulations in LANA-transgenic and LANA-transgenic × CD19-deficient animals[a]						P^b
		$LANA^{-/-}$ $CD19^{-/-}$			$LANA^{+/-}$ $CD19^{-/-}$			
		%	SD	*n*	%	SD	*n*	
Early GC	$B220^+$ PNA^+ IgD^+	0.68	0.65	11	1.53	1.31	7	NS
Late GC	$B220^+$ PNA^+ IgD^-	0.28	0.27	11	1.12	1.73	7	NS
Early GC	$B220^+$ PNA^+ $GL7^-$	0.97	0.73	11	1.89	1.62	7	NS
Late GC	$B220^+$ PNA^+ $GL7^+$	0.96	0.82	11	1.84	1.44	7	NS
Activated	PNA^+ $CD69^+$	4.44	1.6	11	5.53	1.30	7	NS
Activated	$B220^+$ $CD86^+$	6.18	2.10	11	8.56	4.85	7	NS
FO[c]	$B220^+$ $CD21^+$ $CD23^+$	85.7	3.82	6	82.1	4.42	9	NS
MZ	$B220^+$ $CD21^{hi}$ $CD23^-$	2.05	0.45	6	3.46	1.08	9	≤0.01

[a] *n*, Number of animals.
[b] NS, not significant.
[c] FO, follicular.

macrophages (red) and also outside the ring of MZ macrophages (white arrows in Fig. 4D, $CD19^{-/-}$ × LANA). Furthermore, B220 fluorescence was brighter in $CD19^{-/-}$ × LANA compared to wild-type or $CD19^{-/-}$ mice. This phenotype is due to the LANA transgene, since $CD19^{+/-}$ hypomorphic, LANA transgenic mice also have significantly more and brighter B220-positive cells compared to LANA transgene-negative littermates (data not shown).

DISCUSSION

The molecular mechanisms by which KSHV latent genes, such as LANA, lead to B-cell hyperplasia, such as MCD, or frank DLBCL, such as PEL, are poorly understood. A number of mechanisms have been proposed for LANA-dependent cell transformation. These include interactions with the cellular antiapoptotic proteins p53, and pRb, as well as signaling pathways that are involved in proliferation (reviewed in reference 14). Biochemical studies show that LANA protein binds to GSK3β (22), as well as a growing number of cellular transcription factors, and that it activates the human telomerase promoter (2, 3, 12, 30, 33, 43, 53). Microarray analyses found that LANA specifically induced only a very limited number of mRNAs (2, 47). This implies that KSHV LANA activates multiple cellular survival pathways in B cells. This phenotype was recapitulated in the LANA transgenic mice.

We examined B-cell populations of LANA transgenic mice with CD19 deficiency background. LANA rescued the MZ B-cell defect of CD19-deficient mice but not the GC defect of CD19-deficient mice. MZ B cells constitute the first wave of the B-cell response to antigen (reviewed in reference 46). They respond to low-affinity antigen encounter, and their response is short-lived by design. Since they do not necessarily require the multitude of finely tuned B-cell-T-cell interactions that take place within the GC, it is conceivable that the MZ defect in CD19 knockout mice was rescued by inducing an activated state through this viral transcription factor.

Other signaling molecules have been implicated in CD19 signaling and MZ formation. PTEN deletion can rescue the $CD19^{-/-}$ defect completely (6). BAFF:BAFF-R is also required for MZ formation, and canonical NF-κB activity brought about by constitutive active IκB kinase 2 can rescue MZ development in BAFF-$R^{-/-}$ mice (50). However, NF-κB does not complement the $CD19^{-/-}$ defect, i.e., substitute for the tonic BCR signaling that is required for B-cell maturation. Notch-RBP-j is also involved in MZ formation (57), and LANA has been shown to interact with this pathway (11, 33). Finally, and perhaps most consistently, signaling through PI3K-Akt is essential for B-cell survival and BCR signaling in mice (13, 25, 55).

We immunized LANA transgenic mice and found that LANA augmented the primary, BCR-dependent, GC response to (i) acute antigen above control, and (ii) above the level of chronic activation, such as results from inadvertent microbial translocation. This would ensure that cells expressing LANA, i.e., virally infected B cells, are preferentially amplified upon antigen encounter. BCR signal strength is crucial to B-cell proliferation, differentiation, and survival (19, 51, 58). Thus, lowering the BCR signaling threshold provides a novel mechanism for viral persistence in B cells.

Other B-cell-tropic herpesviruses provide examples of mechanistically different scenarios, which nevertheless yield the same result. EBV latent genes also confer a proliferative advantage upon B cells in transgenic mice, and LMP2A enhances B-cell responses *in vivo* (4, 52, 56, 60). This reflects the evolutionary conservation of B-cell signaling and its importance in gammaherpesvirus latency. Conceptually, the progrowth phenotype of the EBV LMP-1 and LMP-2A transgenic mice is easier to comprehend since these two molecules are located in the membrane and impinge on BCR signaling receptor proximately: they bind receptor-associated kinases via SH- or TRAF-binding domains. Our experiments suggest that LANA engages the same signaling pathways, only further downstream, since LANA is localized in the nucleus.

The B-cell-tropic murine herpesvirus 68 (MHV68) encodes a presumptive superantigen (59) and is known to require B-cell proliferation and, of course, LANA, for the establishment of latency (32, 38, 39, 44). The T-cell-tropic herpesvirus saimiri also encodes a superantigen, which is required for oncogenesis in primates (17, 29). MHV68 is known to activate host macrophages (7), which results in protection from certain bacterial pathogens, and there exists an established association between EBV-positive Burkitt lymphoma and malaria, which many believe centers around chronic exposure to parasite antigens

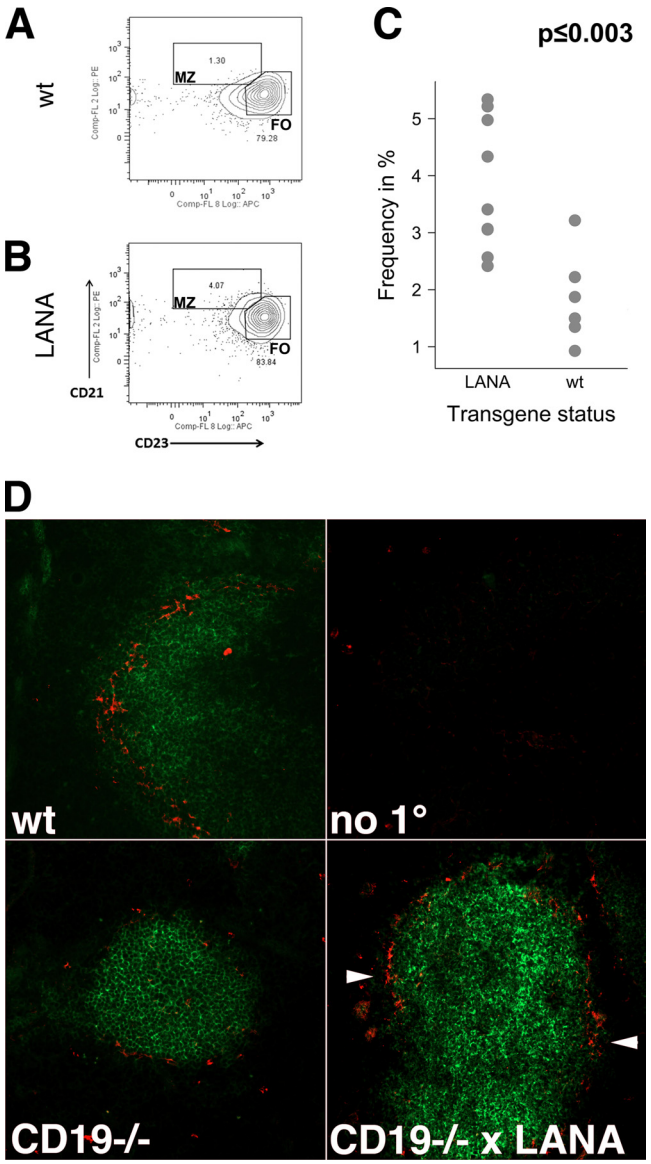

FIG. 4. LANA complements the MZ defect in CD19 knockout mice. (A) Flow cytometry analysis of $B220^+$ B cells in a 15-week-old $LANA^{-/-}/CD19^{-/-}$ mouse spleen. (B) Flow cytometry analysis of $B220^+$ B cells in an age-matched $LANA^{+/-}/CD19^{-/-}$ mouse spleen. (A and B) Gates represent $B220^+$ $CD21^{hi}$ $CD23^-$ MZ B cells. (C) Percentage of MZ B cells ($B220^+$ $CD21^{hi}$ $CD23^-$) in $LANA^{-/-}/CD19^{-/-}$ mice ($n = 6$) and $LANA^{+/-}/CD19^{-/-}$ mice ($n = 9$). (D) Immunofluorescence for MOMA-1 (a marginal zone macrophage marker) in red and B220 (a B-cell marker) in green. The panels show results from wild-type C57BL/6, no-primary-antibody-control, $CD19^{-/-}$, and $LANA^{+/-}/CD19^{-/-}$ mice. Arrowheads indicate that MZ architecture was rescued partially in a $LANA^{+/-}/CD19^{-/-}$ mouse. Magnification, ×200.

(49). Thus, by manipulating B-cell signaling, herpesviruses support the expansion of latent cells.

ACKNOWLEDGMENTS

This study was supported by the National Institutes of Health (CA109232).

We thank B. Vilen and B. Damania for critical reading and Larry Arnold for expert flow cytometry advice.

S.-H.S. performed research, wrote the paper, and analyzed data; F.D.F. performed research; D.P.D. designed research, wrote the paper, and analyzed data.

REFERENCES

1. **Allen, C. D. C., T. Okada, and J. G. Cyster.** 2007. Germinal-center organization and cellular dynamics. Immunity **27:**190–202.
2. **An, F.-Q., N. Compitello, E. Horwitz, M. Sramkoski, E. S. Knudsen, and R. Renne.** 2005. The latency-associated nuclear antigen of Kaposi's sarcoma-associated herpesvirus modulates cellular gene expression and protects lymphoid cells from p16 INK4A-induced cell cycle arrest. J. Biol. Chem. **280:** 3862–3874.
3. **An, J., Y. Sun, and M. B. Rettig.** 2004. Transcriptional coactivation of c-Jun by the KSHV-encoded LANA. Blood **103:**222–228.
4. **Anderson, L. J., and R. Longnecker.** 2009. Epstein-Barr virus latent membrane protein 2A exploits Notch1 to alter B-cell identity in vivo. Blood **113:**108–116.
5. **Ansari, M. Q., D. B. Dawson, R. Nador, C. Rutherford, N. R. Schneider, M. J. Latimer, L. Picker, D. M. Knowles, and R. W. McKenna.** 1996. Primary body cavity-based AIDS-related lymphomas. Am. J. Clin. Pathol. **105:**221–229.
6. **Anzelon, A. N., H. Wu, and R. C. Rickert.** 2003. Pten inactivation alters peripheral B lymphocyte fate and reconstitutes CD19 function. Nat. Immunol. **4:**287–294.
7. **Barton, E. S., D. W. White, J. S. Cathelyn, K. A. Brett-McClellan, M. Engle, M. S. Diamond, V. L. Miller, and H. W. Virgin.** 2007. Herpesvirus latency confers symbiotic protection from bacterial infection. Nature **447:**326–329.
8. **Brenchley, J. M., D. A. Price, and D. C. Douek.** 2006. HIV disease: fallout from a mucosal catastrophe? Nat. Immunol. **7:**235–239.
9. **Carbone, A., E. Cesarman, M. Spina, A. Gloghini, and T. F. Schulz.** 2009. HIV-associated lymphomas and gammaherpesviruses. Blood **113:**1213–1224.
10. **Cesarman, E., Y. Chang, P. S. Moore, J. W. Said, and D. M. Knowles.** 1995. Kaposi's sarcoma-associated herpesvirus-like DNA sequences in AIDS-related body-cavity-based lymphomas. N. Engl. J. Med. **332:**1186–1191.
11. **Chang, H., D. P. Dittmer, Y. C. Shin, Y. Hong, and J. U. Jung.** 2005. Role of Notch signal transduction in Kaposi's sarcoma-associated herpesvirus gene expression. J. Virol. **79:**14371–14382.
12. **Chen, W., I. B. Hilton, M. R. Staudt, C. E. Burd, and D. P. Dittmer.** 2010. Distinct p53, p53:LANA, and LANA complexes in Kaposi's sarcoma-associated herpesvirus lymphomas. J. Virol. **84:**3898–3908.
13. **Dai, X., Y. Chen, J. Schuman, Z. Hua, J. W. Adamson, R. Wen, and D. Wang.** 2006. Distinct roles of phosphoinositide-3 kinase and phospholipase Cγ2 in B-cell receptor-mediated signal transduction. Mol. Cell. Biol. **26:**88–99.
14. **Damania, B., and J. B. Pipas.** 2009. DNA tumor viruses. Springer, New York, NY.
15. **Decker, L., P. Shankar, G. Khan, R. Freeman, B. Dezube, J. Lieberman, and D. Thorley-Lawson.** 1996. The Kaposi sarcoma-associated herpesvirus (KSHV) is present as an intact latent genome in KS tissue but replicates in the peripheral blood mononuclear cells of KS patients. J. Exp. Med. **184:** 283–288.
16. **de Vinuesa, C. G., M. C. Cook, J. Ball, M. Drew, Y. Sunners, M. Cascalho, M. Wabl, G. G. B. Klaus, and I. C. M. MacLennan.** 2000. Germinal centers without T cells. J. Exp. Med. **191:**485–494.
17. **Duboise, M., J. Guo, S. Czajak, H. Lee, R. Veazey, R. C. Desrosiers, and J. U. Jung.** 1998. A role for herpesvirus saimiri orf14 in transformation and persistent infection. J. Virol. **72:**6770–6776.
18. **Dupin, N., C. Fisher, P. Kellam, S. Ariad, M. Tulliez, N. Franck, E. van Marck, D. Salmon, I. Gorin, J.-P. Escande, R. A. Weiss, K. Alitalo, and C. Boshoff.** 1999. Distribution of human herpesvirus-8 latently infected cells in Kaposi's sarcoma, multicentric Castleman's disease, and primary effusion lymphoma. Proc. Natl. Acad. Sci. U. S. A. **96:**4546–4551.
19. **Engel, P., L.-J. Zhou, D. C. Ord, S. Sato, B. Koller, and T. F. Tedder.** 1995. Abnormal B lymphocyte development, activation, and differentiation in mice that lack or overexpress the CD19 signal transduction molecule. Immunity **3:**39–50.
20. **Fakhari, F. D., and D. P. Dittmer.** 2002. Charting latency transcripts in Kaposi's sarcoma-associated herpesvirus by whole-genome real-time quantitative PCR. J. Virol. **76:**6213–6223.
21. **Fakhari, F. D., J. H. Jeong, Y. Kanan, and D. P. Dittmer.** 2006. The latency-associated nuclear antigen of Kaposi sarcoma-associated herpesvirus induces B-cell hyperplasia and lymphoma. J. Clin. Invest. **116:**735–742.
22. **Fujimuro, M., F. Y. Wu, C. ApRhys, H. Kajumbula, D. B. Young, G. S. Hayward, and S. D. Hayward.** 2003. A novel viral mechanism for dysregulation of [beta]-catenin in Kaposi's sarcoma-associated herpesvirus latency. Nat. Med. **9:**300–306.
23. **Han, S., B. Zheng, D. G. Schatz, E. Spanopoulou, and G. Kelsoe.** 1996. Neoteny in lymphocytes: Rag1 and Rag2 expression in germinal center B cells. Science **274:**2094–2097.
24. **Inaoki, M., S. Sato, B. C. Weintraub, C. C. Goodnow, and T. F. Tedder.** 1997. CD19-regulated signaling thresholds control peripheral tolerance and autoantibody production in B lymphocytes. J. Exp. Med. **186:**1923–1931.
25. **Janas, M. L., D. Hodson, Z. Stamataki, S. Hill, K. Welch, L. Gambardella,**

L. C. Trotman, P. P. Pandolfi, E. Vigorito, and M. Turner. 2008. The effect of deleting p110δ on the phenotype and function of PTEN-deficient B cells. J. Immunol. **180:**739–746.
26. **Janeway, C., P. Travers, M. Walport, and M. Shlomchik.** 2001. Immunobiology. Garland Science, London, England.
27. **Jenner, R. G., M. M. Alba, C. Boshoff, and P. Kellam.** 2001. Kaposi's sarcoma-associated herpesvirus latent and lytic gene expression as revealed by DNA arrays. J. Virol. **75:**891–902.
28. **Jeong, J. H., R. Hines-Boykin, J. D. Ash, and D. P. Dittmer.** 2002. Tissue specificity of the Kaposi's sarcoma-associated herpesvirus latent nuclear antigen (LANA/orf73) promoter in transgenic mice. J. Virol. **76:**11024–11032.
29. **Knappe, A., C. Hiller, M. Thurau, S. Wittmann, H. Hofmann, B. Fleckenstein, and H. Fickenscher.** 1997. The superantigen-homologous viral immediate-early gene ie14/vsag in herpesvirus saimiri-transformed human T cells. J. Virol. **71:**9124–9133.
30. **Knight, J. S., M. A. Cotter II, and E. S. Robertson.** 2001. The latency-associated nuclear antigen of Kaposi's sarcoma-associated herpesvirus transactivates the telomerase reverse transcriptase promoter. J. Biol. Chem. **276:**22971–22978.
31. **Kolar, G. R., D. Mehta, R. Pelayo, and J. D. Capra.** 2007. A novel human B-cell subpopulation representing the initial germinal center population to express AID. Blood **109:**2545–2552.
32. **Krug, L. T., J. M. Moser, S. M. Dickerson, and S. H. Speck.** 2007. Inhibition of NF-κB activation in vivo impairs establishment of gammaherpesvirus latency. PLoS Pathog. **3:**e11.
33. **Lan, K., D. A. Kuppers, and E. S. Robertson.** 2005. Kaposi's sarcoma-associated herpesvirus reactivation is regulated by interaction of latency-associated nuclear antigen with recombination signal sequence-binding protein Jκ, the major downstream effector of the Notch signaling pathway. J. Virol. **79:**3468–3478.
34. **Maas, A., G. M. Dingjan, F. Grosveld, and R. W. Hendriks.** 1999. Early arrest in B cell development in transgenic mice that express the E41K Bruton's tyrosine kinase mutant under the control of the CD19 promoter region. J. Immunol. **162:**6526–6533.
35. **Martin, F., A. M. Oliver, and J. F. Kearney.** 2001. Marginal zone and B1 B cells unite in the early response against T-independent blood-borne particulate antigens. Immunity **14:**617–629.
36. **McHeyzer-Williams, M., M. McLean, P. Lalor, and G. Nossal.** 1993. Antigen-driven B-cell differentiation in vivo. J. Exp. Med. **178:**295–307.
37. **Mesri, E., E. Cesarman, L. Arvanitakis, S. Rafii, M. Moore, D. Posnett, D. Knowles, and A. Asch.** 1996. Human herpesvirus-8/Kaposi's sarcoma-associated herpesvirus is a new transmissible virus that infects B cells. J. Exp. Med. **183:**2385–2390.
38. **Moorman, N. J., D. O. Willer, and S. H. Speck.** 2003. The gammaherpesvirus 68 latency-associated nuclear antigen homolog is critical for the establishment of splenic latency. J. Virol. **77:**10295–10303.
39. **Moser, J. M., J. W. Upton, R. D. Allen III, C. B. Wilson, and S. H. Speck.** 2005. Role of B-cell proliferation in the establishment of gammaherpesvirus latency. J. Virol. **79:**9480–9491.
40. **Moser, J. M., J. W. Upton, K. S. Gray, and S. H. Speck.** 2005. Ex vivo stimulation of B cells latently infected with gammaherpesvirus 68 triggers reactivation from latency. J. Virol. **79:**5227–5231.
41. **Otero, D. C., A. N. Anzelon, and R. C. Rickert.** 2003. CD19 function in early and late B-cell development. I. Maintenance of follicular and marginal zone B cells requires CD19-dependent survival signals. J. Immunol. **170:**73–83.
42. **Otero, D. C., and R. C. Rickert.** 2003. CD19 function in early and late B-cell development. II. CD19 facilitates the pro-B/pre-B transition. J. Immunol. **171:**5921–5930.
43. **Ottinger, M., T. Christalla, K. Nathan, M. M. Brinkmann, A. Viejo-Borbolla, and T. F. Schulz.** 2006. Kaposi's sarcoma-associated herpesvirus LANA-1 interacts with the short variant of BRD4 and releases cells from a BRD4- and BRD2/RING3-induced G1 cell cycle arrest. J. Virol. **80:**10772–10786.
44. **Paden, C. R., J. C. Forrest, N. J. Moorman, and S. H. Speck.** Murine gammaherpesvirus 68 LANA is essential for virus reactivation from splenocytes but not long-term carriage of viral genome. J. Virol. **84:**7214–7224.
45. **Paulose-Murphy, M., N.-K. Ha, C. Xiang, Y. Chen, L. Gillim, R. Yarchoan, P. Meltzer, M. Bittner, J. Trent, and S. Zeichner.** 2001. Transcription program of human herpesvirus 8 (Kaposi's sarcoma-associated herpesvirus). J. Virol. **75:**4843–4853.
46. **Pillai, S., and A. Cariappa.** 2009. The follicular versus marginal zone B lymphocyte cell fate decision. Nat. Rev. Immunol. **9:**767–777.
47. **Renne, R., C. Barry, D. Dittmer, N. Compitello, P. O. Brown, and D. Ganem.** 2001. Modulation of cellular and viral gene expression by the latency-associated nuclear antigen of Kaposi's sarcoma-associated herpesvirus. J. Virol. **75:**458–468.
48. **Rickert, R. C., K. Rajewsky, and J. Roes.** 1995. Impairment of T-cell-dependent B-cell responses and B-1 cell development in CD19-deficient mice. Nature **376:**352–355.
49. **Rochford, R., M. J. Cannon, and A. M. Moormann.** 2005. Endemic Burkitt's lymphoma: a polymicrobial disease? Nat. Rev. Microbiol. **3:**182–187.
50. **Sasaki, Y., E. Derudder, E. Hobeika, R. Pelanda, M. Reth, K. Rajewsky, and M. Schmidt-Supprian.** 2006. Canonical NF-κB activity, dispensable for B-cell development, replaces BAFF-receptor signals and promotes B-cell proliferation upon activation. Immunity **24:**729–739.
51. **Sato, S., D. A. Steeber, and T. F. Tedder.** 1995. The CD19 signal transduction molecule is a response regulator of B-lymphocyte differentiation. Proc. Natl. Acad. Sci. U. S. A. **92:**11558–11562.
52. **Shair, K. H., K. M. Bendt, R. H. Edwards, E. C. Bedford, J. N. Nielsen, and N. Raab-Traub.** 2007. EBV latent membrane protein 1 activates Akt, NFκB, and Stat3 in B-cell lymphomas. PLoS Pathog. **3:**e166.
53. **Shamay, M., A. Krithivas, J. Zhang, and S. D. Hayward.** 2006. Recruitment of the de novo DNA methyltransferase Dnmt3a by Kaposi's sarcoma-associated herpesvirus LANA. Proc. Natl. Acad. Sci. U. S. A. **103:**14554–14559.
54. **Song, H., and J. Cerny.** 2003. Functional heterogeneity of marginal zone B cells revealed by their ability to generate both early antibody-forming cells and germinal centers with hypermutation and memory in response to a T-dependent antigen. J. Exp. Med. **198:**1923–1935.
55. **Srinivasan, L., Y. Sasaki, D. P. Calado, B. Zhang, J. H. Paik, R. A. DePinho, J. L. Kutok, J. F. Kearney, K. L. Otipoby, and K. Rajewsky.** 2009. PI3 kinase signals BCR-dependent mature B-cell survival. Cell **139:**573–586.
56. **Swanson-Mungerson, M., R. Bultema, and R. Longnecker.** 2006. Epstein-Barr virus LMP2A enhances B-cell responses in vivo and in vitro. J. Virol. **80:**6764–6770.
57. **Tanigaki, K., H. Han, N. Yamamoto, K. Tashiro, M. Ikegawa, K. Kuroda, A. Suzuki, T. Nakano, and T. Honjo.** 2002. Notch-RBP-J signaling is involved in cell fate determination of marginal zone B cells. Nat. Immunol. **3:**443–450.
58. **Tedder, T. F., M. Inaoki, and S. Sato.** 1997. The CD19-CD21 complex regulates signal transduction thresholds governing humoral immunity and autoimmunity. Immunity **6:**107–118.
59. **Tripp, R. A., A. M. Hamilton-Easton, R. D. Cardin, P. Nguyen, F. G. Behm, D. L. Woodland, P. C. Doherty, and M. A. Blackman.** 1997. Pathogenesis of an infectious mononucleosis-like disease induced by a murine gammaherpesvirus: role for a viral superantigen? J. Exp. Med. **185:**1641–1650.
60. **Uchida, J., T. Yasui, Y. Takaoka-Shichijo, M. Muraoka, W. Kulwichit, N. Raab-Traub, and H. Kikutani.** 1999. Mimicry of CD40 signals by Epstein-Barr virus LMP1 in B lymphocyte responses. Science **286:**300–303.
61. **Wang, Y., S. R. Brooks, X. Li, A. N. Anzelon, R. C. Rickert, and R. H. Carter.** 2002. The physiologic role of CD19 cytoplasmic tyrosines. Immunity **17:**501–514.